

# The molecular mechanism of G<sub>2</sub>/M cell cycle arrest induced by AFB<sub>1</sub> in the jejunum

Heng Yin<sup>1</sup>, Min Jiang<sup>1</sup>, Xi Peng<sup>1,2</sup>, Hengmin Cui<sup>1,2</sup>, Yi Zhou<sup>2</sup>, Min He<sup>2</sup>, Zhicai Zuo<sup>1,2</sup>, Ping Ouyang<sup>2</sup>, Junde Fan<sup>3</sup> and Jing Fang<sup>1,2</sup>

<sup>1</sup> Key Laboratory of Animal Diseases and Environmental Hazards of Sichuan Province, Chengdu, Sichuan, PR China

<sup>2</sup> College of Veterinary Medicine, Sichuan Agricultural University, Chengdu, Sichuan, PR China

<sup>3</sup> College of Biological and Agro-Forestry Engineering, Tongren University, Tongren, Guizhou, PR China

Correspondence to: Jing Fang, email: fangjing4109@163.com

Keywords: AFB<sub>1</sub>; G<sub>2</sub>/M phase; cell cycle arrest; mechanism; jejunum; Pathology Section

Received: March 11, 2016

Accepted: May 12, 2016

Published: May 25, 2016

## ABSTRACT

**Aflatoxin B<sub>1</sub> (AFB<sub>1</sub>) has potent hepatotoxic, carcinogenic, genotoxic, immunotoxic and other adverse effects in human and animals. The aim of this study was to investigate the molecular mechanism of G<sub>2</sub>/M cell cycle arrest induced by AFB<sub>1</sub> in the jejunum of broilers. Broilers, as experimental animals, were fed 0.6 mg/kg AFB<sub>1</sub> diet for 3 weeks. Our results showed that AFB<sub>1</sub> reduced the jejunal villus height, villus height/crypt ratio and caused G<sub>2</sub>/M cell cycle arrest. The G<sub>2</sub>/M cell cycle was accompanied by the increase of ataxia telangiectasia mutated (ATM), p53, Chk2, p21 protein and mRNA expression, and the decrease of Mdm2, cdc25C, cdc2, cyclin B and proliferating cell nuclear antigen protein and mRNA expression. In conclusion, AFB<sub>1</sub> blocked G<sub>2</sub>/M cell cycle by ATM pathway in the jejunum of broilers.**

## INTRODUCTION

Aflatoxins, secondary metabolites produced in feedstuffs by *Aspergillus flavus* and *Aspergillus parasiticus*, which cause health and economic problems when they contaminate food and feed. These mycotoxins are difuranocoumarin compounds and include B<sub>1</sub>, B<sub>2</sub>, G<sub>1</sub>, G<sub>2</sub>, M<sub>1</sub> and M<sub>2</sub> [1]. Of these toxins, aflatoxin B<sub>1</sub> (AFB<sub>1</sub>) is the most commonly encountered and it is considered to have higher toxicity than other aflatoxins. AFB<sub>1</sub> also has potent hepatotoxic, genotoxic, immunotoxic and other adverse effects in many animal species including humans [1, 2-4].

The eukaryotic cell cycle is central to maintain homeostasis in the multicellular organisms [5, 6]. In response to various types of DNA damages, the cell cycle regulatory molecules and cell death signals are activated to stop cell growth and to eliminate multiplication of genetically altered cells [7, 8]. AFB<sub>1</sub> could cause significant increase of S-phase cell population in murine macrophages and human bronchial epithelial cells *in vitro* [9, 10]. In murine models, a significantly greater proportion of lung cells were found to enter cell cycle

with extended S-phase due to AFB<sub>1</sub> treatment [11]. Scott et al. [2] have demonstrated that AFB<sub>1</sub> treatment can lead to an accumulation of chicken thymocytes in G<sub>2</sub>/M phase *in vitro*. Our previous studies suggest that AFB<sub>1</sub> induced jejunal cell arrest at G<sub>2</sub>/M phase and renal cell arrest at G<sub>0</sub>/G<sub>1</sub> phase in broilers [12, 13].

The small intestine is the primary digestive apparatus of animals, and AFB<sub>1</sub> transfer across the gastrointestinal wall is an apparently important step in the fate of the toxin in the animal body [14, 15]. As part of the small intestine, the jejunum is the major component of the gastrointestinal tract. Although there are some studies on cell cycle arrest induced by AFB<sub>1</sub>, few reports focus on the relationship between AFB<sub>1</sub> and cell cycle in the jejunum, and the exact mechanism of G<sub>2</sub>/M cell cycle arrest induced by AFB<sub>1</sub> in jejunum has not been elucidated. To address this, we used a broiler model to examine the effects of dietary AFB<sub>1</sub> in jejunum. We analyzed the histological changes of jejunum, the cell cycle, and the protein and mRNA expression levels of regulatory molecules involved in G<sub>2</sub>/M transition. The results could provide helpful information for the further studies in human and other animals in the future.

## RESULTS

### Pathological observation of jejunum

Compared with the control group, the epithelial cells in the apical region of jejunal villus were shedding in the AFB<sub>1</sub> group at 7, 14 and 21 days of age (Figure 1).

### Villus height, crypt depth and villus/crypt ratio in the jejunum

The villus heights in the AFB<sub>1</sub> group were significantly lower than those in the control group at 14 and 21 days of age ( $p < 0.01$ ), with the exception of villus height on day 7 which did not show a significant decrease in comparison to that in the control group ( $p > 0.05$ ). The

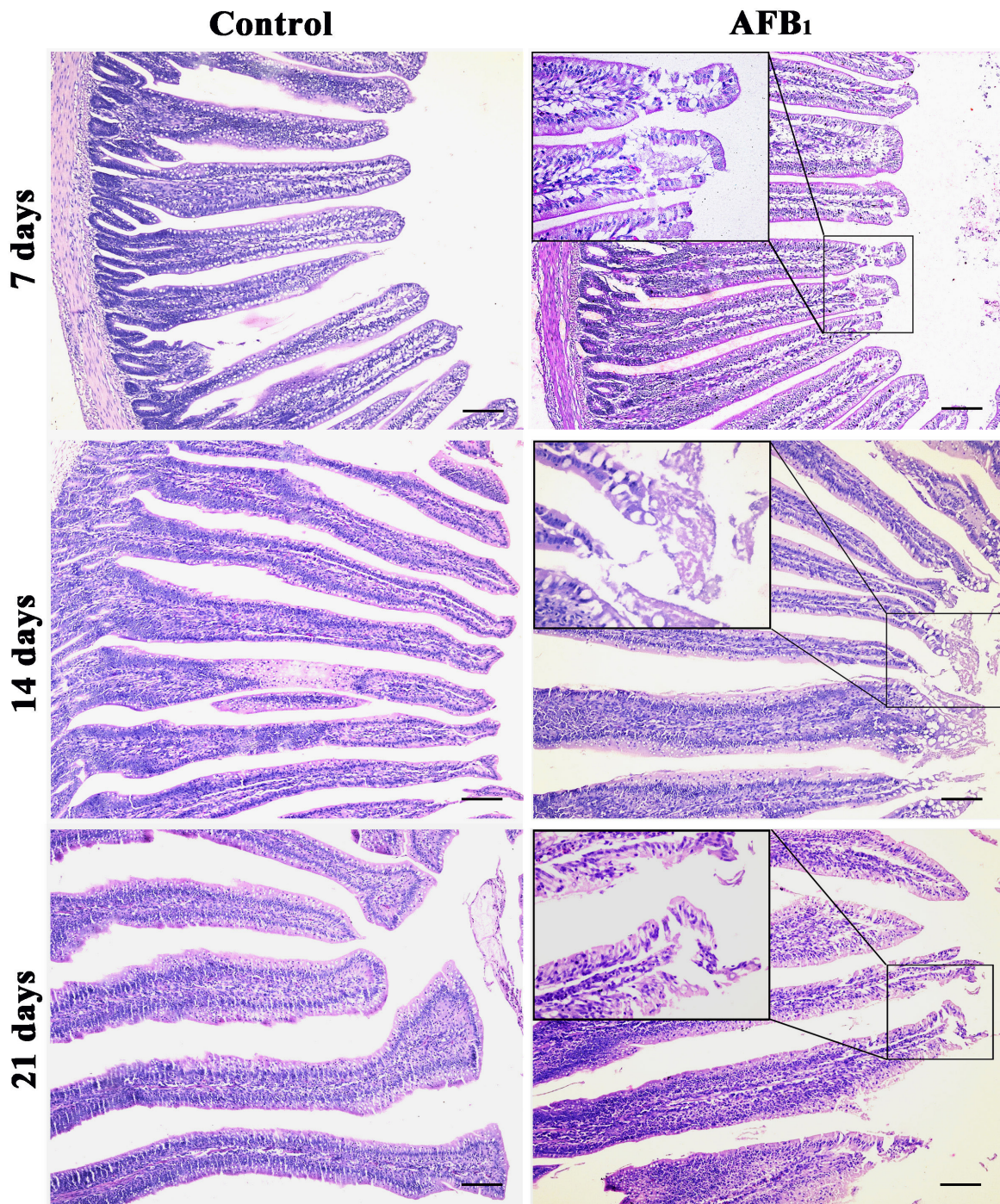


Figure 1: Histological structures of jejunum at 7, 14 and 21 days of age (H.E staining, scale bar: 100  $\mu$ m).

crypt depth in the AFB<sub>1</sub> group significantly increased at 7, 14 and 21 days of age ( $p < 0.05$  or  $0.01$ ), when compared with that in the control group. In addition, the villus/crypt ratios in the AFB<sub>1</sub> group were significantly lower than those in the control group at 7, 14 and 21 days of age ( $p < 0.01$ ) (Figure 2).

### Cell cycle in the jejunal mucosa

The percentage of cells in G<sub>0</sub>/G<sub>1</sub> phase was significantly lower in the AFB<sub>1</sub> group than that in the control group at 21 days of age ( $p < 0.05$ ), but the change was not obvious at 7 and 14 days of age ( $p > 0.05$ ). The cell percentages of G<sub>2</sub>/M phase were significantly higher in the AFB<sub>1</sub> group than those in the control group at 7, 14 and 21 days of age ( $p < 0.01$ ). No significant differences in cell percentage of S phase were noted between two groups at 7, 14 and 21 days ( $p > 0.05$ ) (Figure 3).

### Expression of cell cycle regulatory molecule proteins by immunohistochemistry

Stained brownish-yellow, the expression of G<sub>2</sub>/M cell cycle regulatory molecule proteins is shown in Figure 4, 5 and 6. Control sections showed negative reaction (Figure 5).

The p-ATM protein expression was significantly increased ( $p < 0.01$ ) in the AFB<sub>1</sub> group at 7, 14 and 21 days of age, when compared with those in the control group. The p53 and p21 protein expression were significantly higher ( $p < 0.01$ ) in the AFB<sub>1</sub> group at 7, 14 and 21 days of age than those in the control group. But compared with the control group, the PCNA protein expression in the AFB<sub>1</sub> group was significantly decreased at 7, 14 and 21 days of age ( $p < 0.05$  or  $0.01$ ) (Figure 6).

The p-Chk2 protein expression was significantly higher ( $p < 0.01$ ) in the AFB<sub>1</sub> group than that in the control group from 7 to 21 days of age. The p-cdc25C and cyclin B protein expression were significantly decreased ( $p < 0.01$ ) in the AFB<sub>1</sub> group at 7, 14 and 21 days of age compared with those in the control group (Figure 6).

### The expression of cell cycle regulatory mRNA by qRT-PCR

When compared with the control group, the mRNA expression levels of ATM, Chk2 and CyclinB<sub>3</sub> in the AFB<sub>1</sub> group were obviously increased at 7, 14 and 21 days of age ( $p < 0.05$  or  $0.01$ ). The mRNA expression of cdc25 was decreased at 14 and 21 days of age ( $p < 0.01$ ), but not significantly dropped at 7 days of age ( $p > 0.5$ ). And the expression levels of cdc2 mRNA in the AFB<sub>1</sub> group were obviously decreased at 7 and 21 days of age ( $p < 0.05$  or  $0.01$ ), but not significantly changed at 14 days of

age compared with the control group ( $p > 0.5$ ) (Figure 7).

The mRNA expression of p53 and p21 was obviously increased at 7, 14 and 21 days of age after exposure to AFB<sub>1</sub> ( $p < 0.05$  or  $0.01$ ). The mRNA expression of Mdm2 and PCNA became significantly decreased at 7, 14 and 21 days of age compared with those of the control group ( $p < 0.01$ ) except for PCNA (Figure 7).

## DISCUSSION

According to previous [12] and present researches, AFB<sub>1</sub> retarded the development of jejunum, including the shedding of villus and the reduction of the villus height and villus height/crypt ratio, which may be dependent on the decreased abilities of cell proliferation. As we know, the shedding of villus should be responsible for lower villus height. However, significant lower villus heights were observed in the AFB<sub>1</sub> group at 14 and 21 days and not at 7 days in this study. The reason for this may be complicated because villus growth involves epithelial cell proliferation rates, migration rates of epithelial cells from the crypts to the villus tip, or apoptosis and exfoliation rates of epithelial cells [16]. Therefore, besides shedding, other factors may also be responsible for lower villus height. In addition, the morphological modifications reported in Figure 1 were that the epithelial cells in the apical region of jejunal villus were shedding. As reported in Figure 3 lower percentage of cells in G<sub>0</sub>/G<sub>1</sub> is observed only at 21 days and is only minor in the AFB<sub>1</sub> group. This means that cell proliferation is lightly increased. The possible relevance of these changes to the morphological modifications reported in Figure 1 is that the enhancement of cell proliferation might be attributed to the repair ability due to the continuous damage to the epithelial cells which is the protective mechanism of the organism. But the key finding is that AFB<sub>1</sub> induced jejunal cell cycle arrest at the G<sub>2</sub>/M phase, which was in line with our earlier research [12]. However, the mechanism of G<sub>2</sub>/M cell cycle arrest induced by AFB<sub>1</sub> is unclear.

In this present study, the G<sub>2</sub>/M phase cell cycle regulatory molecules were measured in order to define the molecular mechanism of AFB<sub>1</sub>-induced G<sub>2</sub>/M phase arrest in broiler's jejunum. The ataxia telangiectasia mutated (ATM) plays a critical role in the activation of cell cycle checkpoints [17]. The ATM pathway responds mainly to DNA double strand breaks but also to other types of DNA damage [18]. The central position of ATM in the maintenance of genomic stability becomes apparent by its involvement in checkpoint regulation at the G<sub>2</sub>/M transition [19, 20]. At the DNA-damage, ATM activates Chk2 by phosphorylation [21], and then the Chk2 influences the stabilization of p53 [22]. Chk2 can induce G<sub>2</sub>/M cell cycle arrest through p53 up-regulation [22, 23]. Furthermore, AFB<sub>1</sub> is metabolized to aflatoxin-8, 9-epoxide by cytochrome P450 (CYP450) microsomal

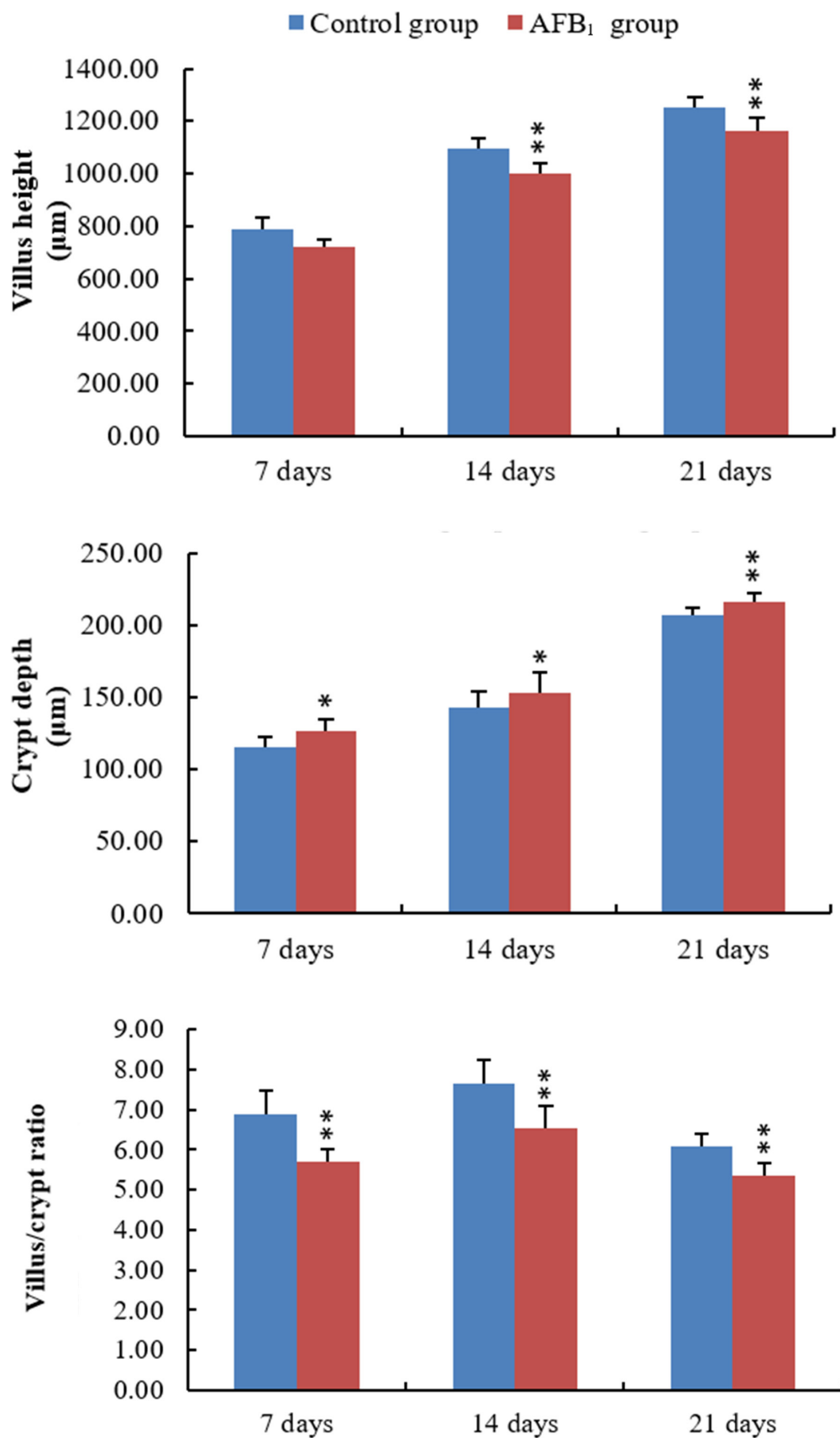


**Figure 2: The values of villus height, crypt depth and villus/crypt ratio in the jejunum.** Note: data are presented with the means ± standard deviation ( $n = 6$ ). \* $p < 0.05$ , \*\* $p < 0.01$  compared with control group.

enzymes, and the reactive aflatoxin-8, 9-epoxide can cause DNA damage [24]. In the present study, our results showed that AFB<sub>1</sub> caused the increase of ATM, p-Chk2

and p53 protein and mRNA expression, suggesting that AFB<sub>1</sub> activated the ATM signal transduction pathways by up-regulation of ATM, Chk2 and p53. Therefore, AFB<sub>1</sub>

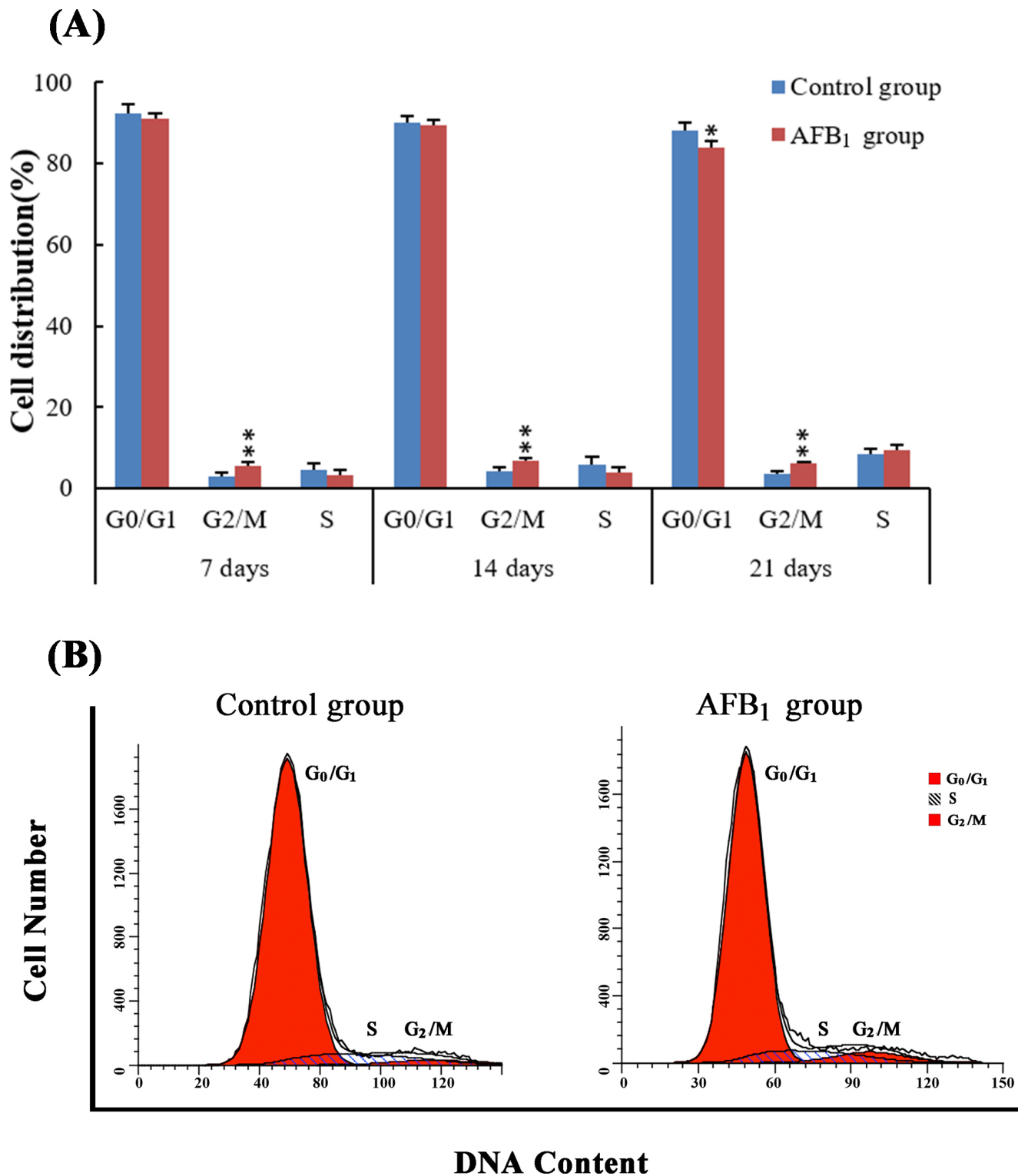


**Figure 3: The cell cycle of jejunal mucosa by flow cytometry.** Panel A: Percentage of cells in G<sub>0</sub>/G<sub>1</sub>, S and G<sub>2</sub>/M phases. Data are presented with the means ± standard deviation (*n* = 6) \**p* < 0.05, \*\**p* < 0.01 compared with control group. Panel B: Flow cytometric analysis of cell cycle distribution in the jejunal mucosa cells at 14 days of age, showing cell cycle arrest in G<sub>2</sub>/M phase induced by AFB<sub>1</sub>.

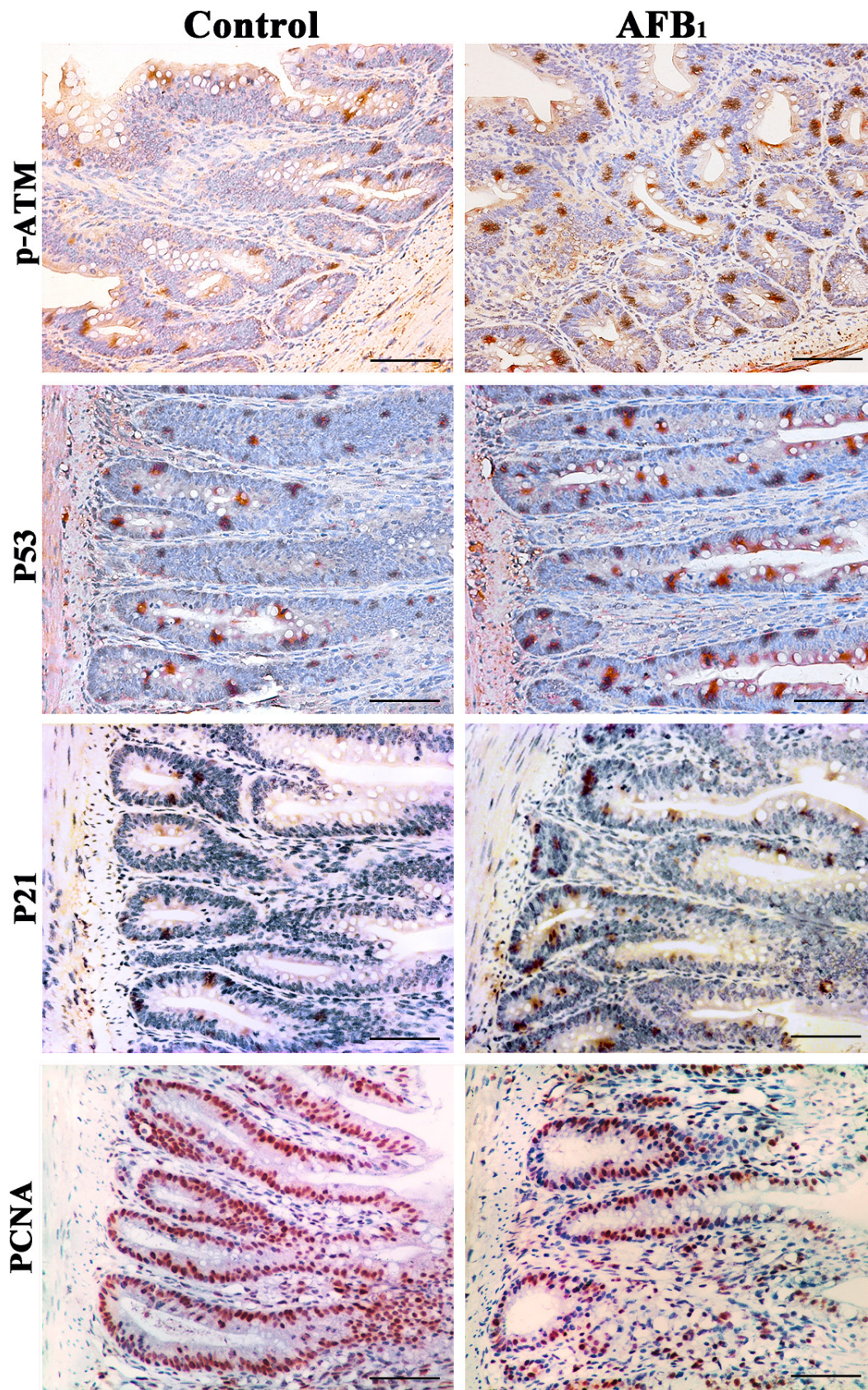


Figure 4: Expression of p-ATM, p53, p21 and PCNA protein in the jejunum at 14 days of age (Immunohistochemistry, scale bar: 50µm).

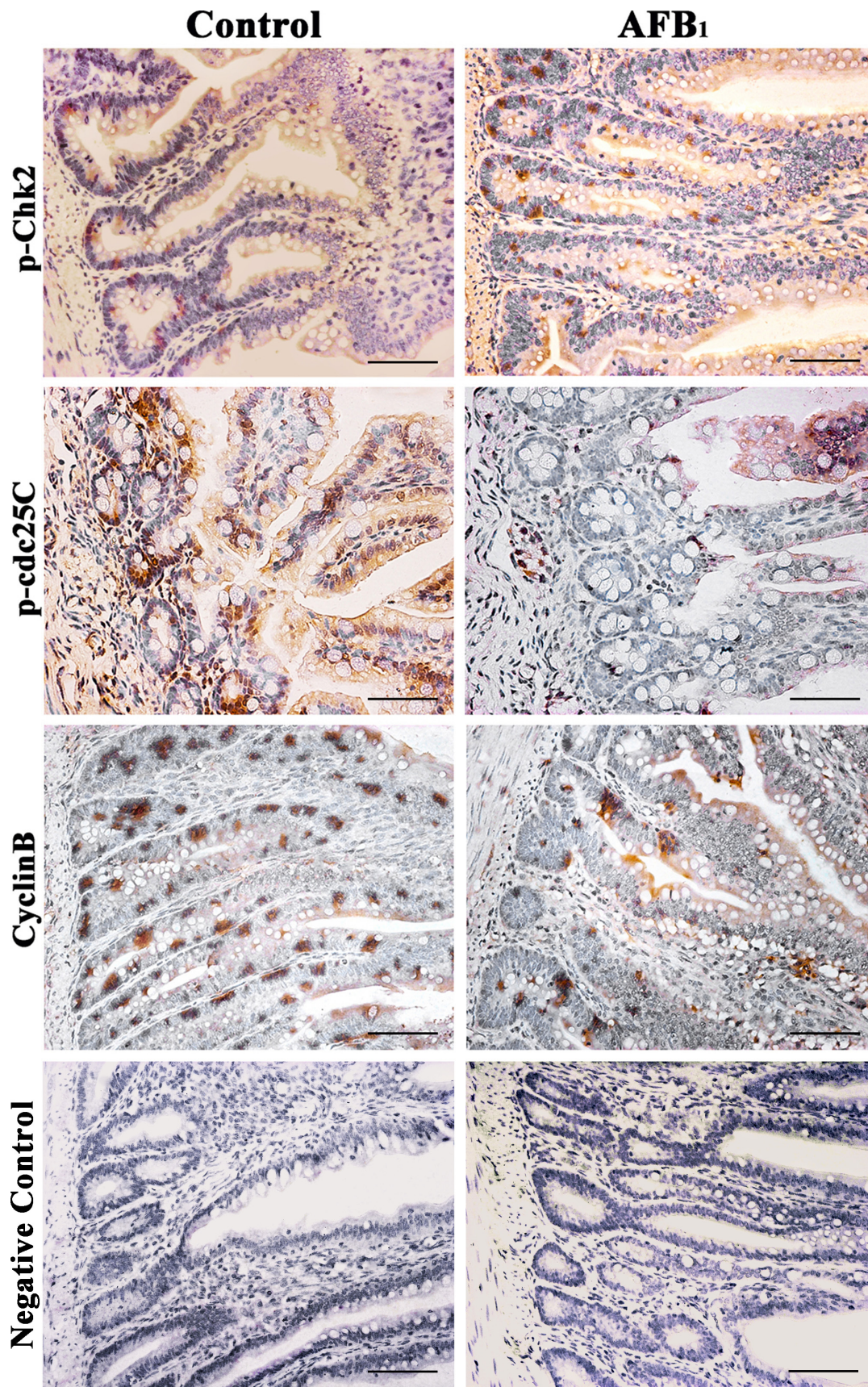
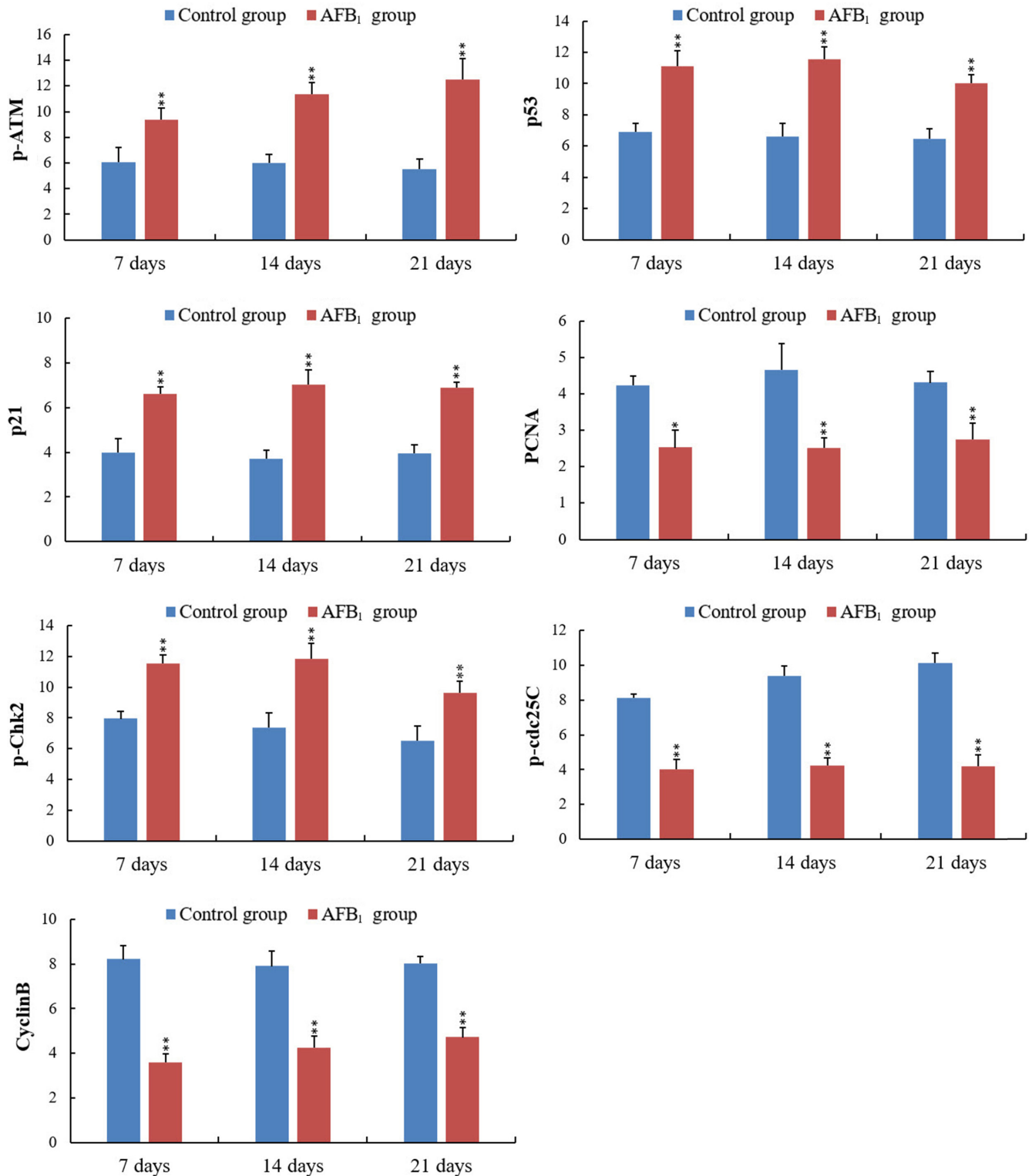


Figure 5: Expression of p-Chk2, p-cdc25C and cyclinB protein in the jejunum at 14 days of age (Immunohistochemistry, scale bar: 50µm).

induced G<sub>2</sub>/M cell cycle arrest *via* two different routes: the ATM-p53 and the ATM-Chk2 pathways. Similarly, Yang

et al. [10] reported that ATM, ATR, Chk2 and p53 were up-regulated by AFB<sub>1</sub> in B-2A13 cells. Gursoy-Yuzugullu



**Figure 6: Integrated optical density (IOD) of p-ATM, p53, p21, PCNA, p-Chk2, p-cdc25C and CyclinB protein expression in the jejunum.** Note: Data are presented with the mean ± standard deviation (n = 6). \*p < 0.05, \*\*p < 0.01 compared with the control group.



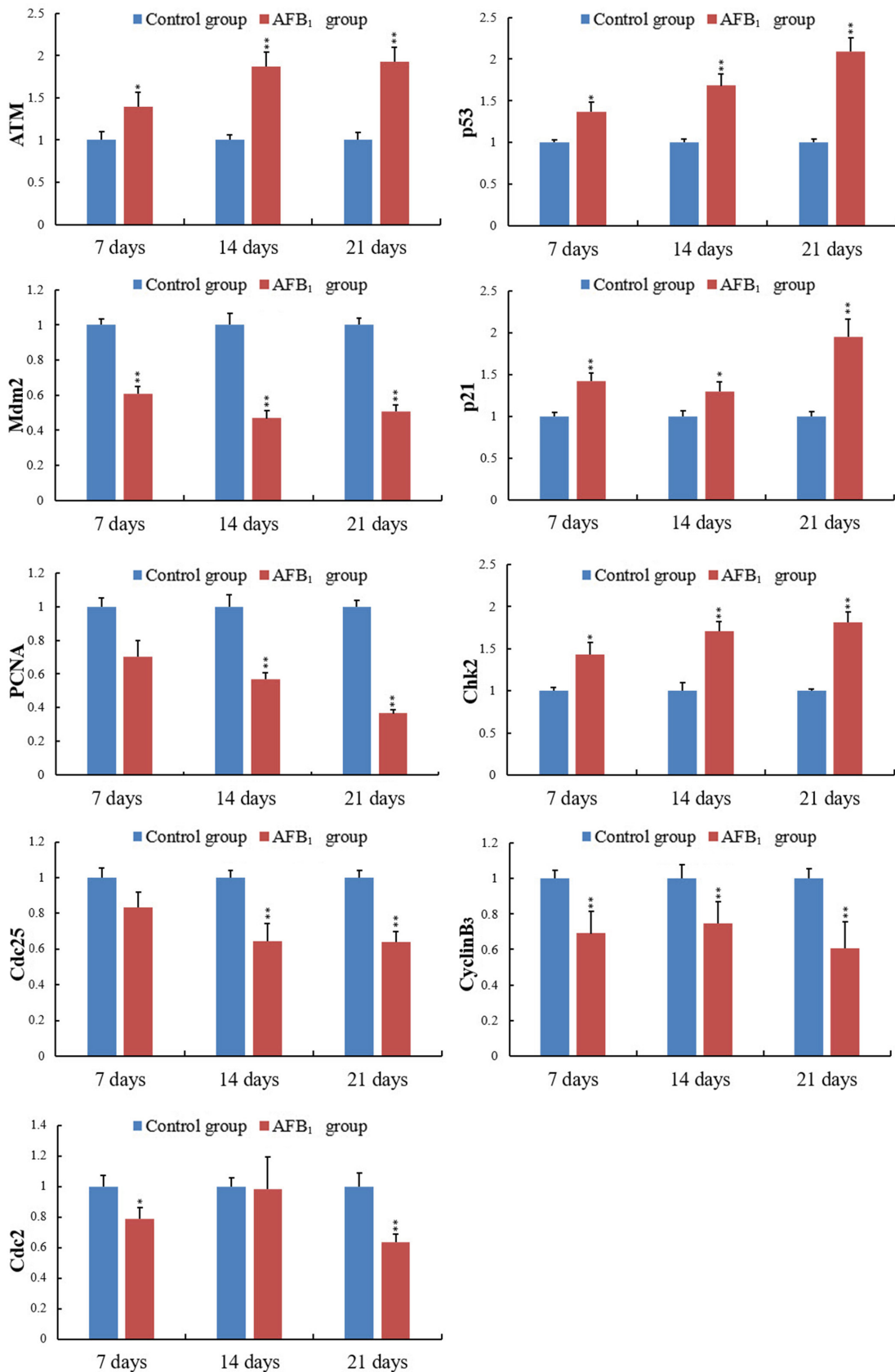


**Figure 7: The levels of the ATM, Chk2, cdc25, CyclinB3, cdc2, mdm2, p53, p21 and PCNA mRNA expression in the jejunal mucosa.** Note: Data are presented with the mean  $\pm$  standard deviation ( $n = 6$ ). \* $p < 0.05$ , \*\* $p < 0.01$  compared with the control group.

et al. [25] found that AFB<sub>1</sub> induced accumulation of p53 in HepG2 hepatoma cells.

P53 is a crucial mediator of at least two or more cellular responses to a variety of DNA damage: apoptosis, DNA repair and cell cycle arrest [26]. In normal conditions, p53 levels are low due to continuous Mdm2-mediated ubiquitination and degradation, and the activation of Mdm2 by p53 is required to reverse the inhibitory effects of p53 on cell cycle progression [27]. P53 can induce p21 up-regulation, which causes cells to arrest in G<sub>2</sub>/M phase [28]. Furthermore, p21 induces cell cycle arrest at G<sub>2</sub>/M phase by inhibiting cdc2 [29, 30]. An inactive cdc2/cyclin B complex does not allow cells to progress beyond the G<sub>2</sub>/M cell-cycle checkpoint. Meanwhile, p21 inhibits DNA replication and maintains G<sub>2</sub>/M cell cycle arrest through the binding to PCNA and the reduction of PCNA [31-33]. The PCNA, as a marker of proliferation, takes part in DNA biological synthesis and regulates cell cycle [34, 35]. The limitation of cdc2/cyclin B complex formation and the down-regulation of

PCNA expression block the passage of cells to mitosis [31, 36]. In this study, our results showed that AFB<sub>1</sub> caused the increase of p53 and p21 proteins and mRNA expression, and decrease of cyclin B and PCNA protein and mRNA expression as well as cdc2 and Mdm2 mRNA expression. Therefore, we speculated that dietary AFB<sub>1</sub> could cause G<sub>2</sub>/M cell cycle arrest in jejunum through p53-dependent p21 activation. Similar results were also observed in the following references. β-Mangostin can induce the p53-dependent G<sub>2</sub>/M cell cycle arrest by down-regulating cdc2 and PCNA [37]. Exposure of HEK 293 cells to citrinin induced cell cycle G<sub>2</sub>/M arrest and increased the expression of p53 and p21 proteins [38]. Deoxynivalenol arrested epithelial cell cycle at G<sub>2</sub>/M phase *via* elevated p21 gene expression [39]. In human liver cells, Ochratoxin A (OTA) exerted a major influence on G<sub>2</sub> phase arrest, in which the cyclin B1-cdc2 complex was reduced and the expression of cdc2 and cyclin B1 were significantly decreased by OTA treatment both at protein and mRNA level [40].

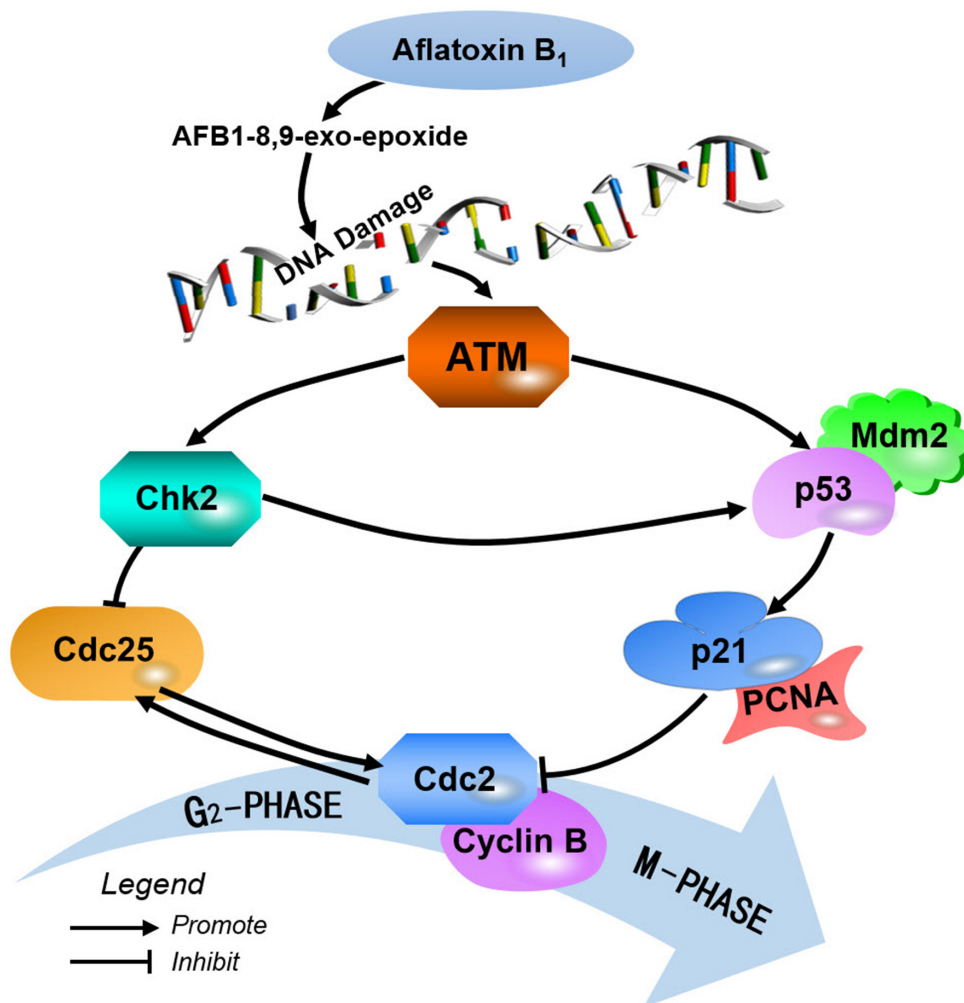


**Figure 8:** Schematic diagram of the proposed the molecular mechanism of aflatoxin B1 arrest G2/M cell cycle in broiler's jejunum.

**Table 1: Antibodies used in immunohistochemistry**

Name	Company	Cat#	Source	Dilution
p-ATM	Bioss, China	bs-2272R	Rabbit	1:100
p-Chk2	Bioss, China	bs-3721R	Rabbit	1:100
p53	Boster, China	BM0101	Mouse	1:100
p21	Boster, China	BA0272	Rabbit	1:100
p-cdc25C	Bioss, China	bs-3482R	Rabbit	1:100
Cyclin B1	Boster, China	BA0766	Rabbit	1:100
PCNA	Bioss, China	bs-0754R	Rabbit	1:100

Herein, up-regulation of Chk2 protein and mRNA expression indicates that AFB<sub>1</sub> activates ATM-Chk2 pathways to inhibit cdc2/cyclin B expression. The cyclin B/cdc2 complexes are also activated in prophase by the cdc25 phosphatase, while inhibition of cdc25 by the checkpoint kinases Chk2 prevents cyclin B/cdc2 activation [41, 42]. And the relatively low amounts of the formation of an active cyclin B/Cdc2 complex may be the main factor of cells accumulated in G<sub>2</sub>/M phase [43]. Our results showed that AFB<sub>1</sub> caused the decrease of cdc25C expression, indicating that AFB<sub>1</sub> induced G<sub>2</sub>/M phase arrest *via* ATM-Chk2-cdc25-cyclin B/cdc2 route.

In summary, 0.6 mg/kg AFB<sub>1</sub> in the diet inhibited the development of broiler's jejunum by causing G<sub>2</sub>/M cell cycle arrest. This was accompanied by the increase of ATM, p53, p21 and Chk2 proteins and mRNA expression, and the decrease of cdc25, cdc2, cyclin B, Mdm2 and PCNA proteins and mRNA expression. Here, we showed the proposed mechanisms of jejunal G<sub>2</sub>/M cell cycle arrest caused by AFB<sub>1</sub> (Figure 8).

## MATERIALS AND METHODS

### Experimental design

One hundred and fifty-six one-day-old healthy Cobb broilers were randomly divided into two groups with three replicates per group and 26 birds per replicate, namely control group (0 mg/kg AFB<sub>1</sub>) and AFB<sub>1</sub> group (0.6 mg/kg AFB<sub>1</sub>). The use of broilers and all experimental procedures involving animals were approved by Sichuan Agricultural University Animal Care and Use Committee. Nutritional requirements were adequate according to National Research Council (1994) (National Research Council, 1994) [44] and Chinese Feeding Standard of Chicken (NY/T33-2004). AFB<sub>1</sub> was obtained from Sigma-Aldrich (USA, A6636). The AFB<sub>1</sub>-contaminated diet was made, similarly to the method described by Kaoud [45]. Briefly, 27 mg AFB<sub>1</sub> farinose solid was dissolved into 30 mL methanol completely, and then the 30 mL mixture was mixed into 45 kg corn-soybean basal diet to formulate AFB<sub>1</sub> diet of experimental groups containing 0.6mg/kg AFB<sub>1</sub>. The equivalent methanol was mixed into corn-soybean basal

diet to produce control diet. Then, the methanol of diets was evaporated at 98 °F (37 °C). The AFB<sub>1</sub> concentrations were analyzed by HPLC (Waters, Milford, MA, USA ) with fluorescence detection (Waters, Model 2475, Milford, MA, USA), and the AFB<sub>1</sub> concentrations were determined as < 0.01mg/kg and 0.061mg/kg in the control diet and AFB<sub>1</sub> diet, respectively. Broilers were housed in cages with electrically heated units and provided with water as well as above mentioned diet *ad libitum* for 21 days.

### Histopathological examination

At the end of 7, 14 and 21 days of experiment, six chickens in each group were euthanized, and jejunum (the midpoint between the bile duct entry and Meckel's diverticulum) were immediately fixed in 4% paraformaldehyde. After fixation for 24 h, tissues were dehydrated, paraffin embedded, sectioned at 5 μm, and stained with haematoxylin and eosin (H.E) for histological examination. Paraffin sections were also collected to perform immunohistochemistry. The histological structures of the tissues were observed and photographed with a digital camera (Nikon DS-Ri1, Japan). Altogether 10 measurements were taken per broiler for each parameter in the jejunum stained with H.E using Image-Pro Plus 5.1 (USA) image analysis software. The following parameters were determined: the villus height (length from the tip of the villus to the crypt mouth), crypt depth (length from the crypt mouth to the crypt base following the crypt lumen) and villus height to crypt depth (villus/crypt) ratio.

### Cell cycle analysis by flow cytometry

At the end of 7, 14 and 21 days, six chickens in each group were selected for the determination of the cell cycle stages in jejunum by flow cytometry, with a similar method described by Chen et al. [46]. Briefly, the chickens were humanely killed and the jejunal mucosae were obtained, and minced using scissors to form a cell suspension that was filtered through a 300-mesh nylon screen. The cells were washed twice with ice-cold phosphate buffer saline (PBS, pH 7.2-7.4), and then suspended in PBS at a concentration of 1 × 10<sup>6</sup> cells/mL. A total of 500 μL of the cell suspension was transferred to a 5-mL culture tube.

**Table 2: Sequence of primers used in qRT-PCR**

Gene symbol	Accession number	Primer	Primer sequence(5'-3')	Product size	Tm (°C)
ATM	NM001162400.1	Forward Reverse	TTGCCCACTCTTTCCATGT CCCCTGCATATTCCTCCAT	110bp	60
Chk2	NM001080107	Forward Reverse	AGACCAAATCACTCGTGGAGAATAC GATGCTCTAAGGCTTCTCTATTGT	140bp	60
cdc25	NM001199572.1	Forward Reverse	AGCGAAGATGATGACGGATT GCAGAGATGAAGAGCCAAAGA	163bp	59
p53	NM205264.1	Forward Reverse	ACCTGCACTTACTCCCCGGT TCTTATAGACGGCCACGGCG	127bp	59
Mdm2	AF005045.1	Forward Reverse	AACTTCCCAGCCAACAACA TCAAAGGTCAACGAGATGCT	123bp	59
p21	AF513031.1	Forward Reverse	TCCCTGCCCTGTACTGTCTAA GCGTGGGCTCTTCTTATACAT	123bp	60
cdc2	NM205314.1	Forward Reverse	TCTGCTCTGTATTCCACTCCTG ATTGTTGGGTGTCCCTAAAGC	144bp	60
cyclinB3	NM205239.2	Forward Reverse	ATCACCAACGCTCACAAGAAC AGGCTCCACAGGAACATCTG	171bp	59
PCNA	AB053163.1	Forward Reverse	GATGTTCTCTCGTTGTGGAG CAGTGCAGTTAAGAGCCTTCC	104bp	60
β-actin	L08165	Forward Reverse	TGCTGTGTTCCCATCTATCG TTGGTGACAATACCGTGTCA	178bp	62

After centrifugation (200×g, 5 min), the supernatant was separated, the cells were incubated for 30 min at room temperature in the dark with 5 μL 0.25% Triton X-100 and 5 μL Propidium Iodide (PI) (Cat. No.51-66211E). Finally, 500 μL of PBS were added to each tube, and cells were analyzed by flow cytometry (BD FACSCalibur) within 45 min of preparation. The results of cell cycle were analyzed using the Mod Fit LT for Mac V3.0 computer program.

### Immunohistochemistry

The method of immunohistochemistry was applied according to the report by Fang et al. [47]. The jejunal paraffin sections were dewaxed in xylene, rehydrated through a graded series of ethanol solutions, washed in distilled water and PBS and endogenous peroxidase activity was blocked by incubation with 3% H<sub>2</sub>O<sub>2</sub> in methanol for 15 min. The sections were saturated with normal 10% goat sera for 30 min in order to eliminate non specific irrelevant proteins staining and then incubated with the primary(rabbit/mouse)antibodies (Table 1) for 17 h at 4 °C (working dilution: 1:100). After washing in PBS, the slices were exposed to 1% biotinylated goat anti-rabbit/mouse IgG secondary antibody (Boster, Wuhang, China)

for 1 h at 37 °C, and then incubated with strept avidin-biotin complex (SABC; Boster, Wuhang, China) for 30 min at 37 °C. To visualize the immunoreaction, sections were immersed in diaminobenzidine hydrochloride (DAB; Boster, Wuhang, China). The slices were monitored microscopically and stopped by immersion in distilled water, as soon as brown staining was visible. Slices were lightly counterstained with hematoxylin, dehydrated in ethanol, cleared in xylene and mounted. For negative control purposes, representative sections were processed in the same way by replacing primary antibodies by PBS.

In this study, the protein expression levels of the cell cycle regulatory molecules were determined by the integrated optical density (IOD). Briefly, photographs of the jejunums were taken with a digital microscope camera system (Nikon DS-Ri1, Japan). For each section, five fields of 0.064 mm<sup>2</sup> from each area of the image were analyzed using computer-assisted image-Pro Plus 5.1 (USA) image analysis software. By selecting “colour-chosen target” in the option bar of the morphologic analysis system, all positive immunoreactive cells in the field were marked in colour. Then, “calculating” in the option bar was selected to automatically calculate the IOD value.

## Quantitative real-time PCR

The jejunal mucosae from six chickens in each group were taken at 7, 14 and 21 days of age and stored in liquid nitrogen. The jejunal mucosae were crushed with pestle to homogenize until powdery, respectively. As previously described [48], total RNA was extracted from the powdery of jejunal mucosae using RNAiso Plus (9108/9109, Takara, Otsu, Japan). Next, cDNA was synthesized using a Prim-Script™ RT reagent Kit (RR047A, Takara, Japan) according to the manufacture's protocol. The cDNA product was used as a template for qRT-PCR analysis. Sequences for target genes were obtained from the NCBI database. Oligonucleotide primers were designed using Primer 5 software and synthesized at Takara (Dalian, China; Table 2). All qRT-PCR were performed using the SYBR® Premix Ex Taq™ II system (DRR820A, Takara, Japan) using on a Model C1000 Thermal Cycler (Bio Rad, USA). Chicken  $\beta$ -actin expression was used as an internal reference housekeeping gene. Gene expression values from control group subsamples at 7, 14, and 21 days of age were used to calibrate gene expression in subsamples from corresponding experimental subsamples. All data output from the qRT-PCR experiments were analyzed using the  $2^{-\Delta\Delta CT}$  method [49].

## Statistical analysis

The significance of difference between two groups was analyzed by variance analysis, and results were expressed as mean  $\pm$  standard deviation ( $\bar{X} \pm SD$ ). The analysis was performed using the independent sample test of SPSS 20.0 software (IBM Corp, Armonk, NY, USA) for windows. Statistical significance was considered at  $p < 0.05$  and markedly significant was considered at  $p < 0.01$ .

## ACKNOWLEDGMENTS

This work was supported by the program for Changjiang scholars, the University Innovative Research Team (IRT 0848) and the Education Department of Sichuan Province (2012FZ0066) and (2013FZ0072).

## CONFLICTS OF INTEREST

The authors declare no conflict of interest.

## REFERENCES

1. Yunus AW, Razzazi-Fazeli E and Bohm J. Aflatoxin B1 in affecting broiler's performance, immunity, and gastrointestinal tract: A review of history and contemporary issues. *Toxins*. 2011; 3:566-590.
2. Scott TR, Rowland SM, Rodgers RS and Bodine AB.

- Genetic selection for aflatoxin B 1 resistance influences chicken T-cell and thymocyte proliferation. *Dev Comp Immunol*. 1991; 15:383-391.
3. Abbès S, Salah-Abbès JB, Abdel-Wahhab MA and Ouslati R. Immunotoxicological and biochemical effects of Aflatoxins in rats prevented by Tunisian Montmorillonite with reference to HSCAS. *Immunopharm Immunot*. 2010; 32:514-522.
4. Kalpana S, Aggarwal M, Rao GS and Malik JK. Effects of aflatoxin B1 on tissue residues of enrofloxacin and its metabolite ciprofloxacin in broiler chickens. *Environ Toxicol Phar*. 2012; 33:121-126.
5. Hartwell LH and Kastan MB. Cell cycle control and cancer. *Science*. 1994; 266:1821-1828.
6. Schafer K. The cell cycle: a review. *Vet Pathol*. 1998; 35:461-478.
7. O'connor P. Mammalian G1 and G2 phase checkpoints. *Cancer Surv*. 1996; 29:151-182.
8. Branzei D and Foiani M. Regulation of DNA repair throughout the cell cycle. *Nat Rev Mol Cell Bio*. 2008; 9:297-308.
9. Bianco G, Russo R, Marzocco S, Velotto S, Autore G and Severino L. Modulation of macrophage activity by aflatoxins B1 and B2 and their metabolites aflatoxins M1 and M2. *Toxicon*. 2012; 59:644-650.
10. Yang X, Zhang Z, Wang X, Wang Y, Zhang X, Lu H and Wang S-L. Cytochrome P450 2A13 enhances the sensitivity of human bronchial epithelial cells to aflatoxin B1-induced DNA damage. *Toxicol Appl Pharmacol*. 2013; 270:114-121.
11. Raj HG, Gupta K, Rohil V, Bose M, Biswas G, Singh SK, Jain SC, Parmar VS, Olsen CE and Wengel J. Aflatoxin B1-induced micronuclei and cell cycle alterations in lung and bone marrow cells and their modulation by Piper argyrophyllum extract. *Teratogen Carcin Mut*. 1998; 18:249-261.
12. Zhang S, Peng X, Fang J, Cui H, Zuo Z and Chen Z. Effects of Aflatoxin B1 Exposure and Sodium Selenite Supplementation on the Histology, Cell Proliferation, and Cell Cycle of Jejunum in Broilers. *Biol Trace Elem Res*. 2014; 160:32-40.
13. Yu Z, Wang F, Liang N, Wang C, Peng X, Fang J, Cui H, Mughal MJ and Lai W. Effect of Selenium Supplementation on Apoptosis and Cell Cycle Blockage of Renal Cells in Broilers Fed a Diet Containing Aflatoxin B1. *Biol Trace Elem Res*. 2015; 168:242-251.
14. Kumagai S. Intestinal absorption and excretion of aflatoxin in rats. *Toxicol Appl Pharmacol*. 1989; 97:88-97.
15. Schultz SG. Small Intestinal Absorption. *Role Gastrointestinal Tract Nutrient Del*. 2012; 3:119.
16. De Conto C, Oevermann A, Burgener I, Doherr M and Blum J. Gastrointestinal tract mucosal histomorphometry and epithelial cell proliferation and apoptosis in neonatal and adult dogs. *J Anim Sci*. 2010; 88:2255-2264.16.

17. Kurz EU and Lees-Miller SP. DNA damage-induced activation of ATM and ATM-dependent signaling pathways. *DNA Repair*. 2004; 3:889-900.
18. Sancar A, Lindsey-Boltz LA, Ünsal-Kaçmaz K and Linn S. Molecular mechanisms of mammalian DNA repair and the DNA damage checkpoints. *Annu Rev Biochem*. 2004; 73:39-85.
19. Kudoh A, Fujita M, Zhang L, Shirata N, Daikoku T, Sugaya Y, Isomura H, Nishiyama Y and Tsurumi T. Epstein-Barr virus lytic replication elicits ATM checkpoint signal transduction while providing an S-phase-like cellular environment. *J Biol Chem*. 2005; 280:8156-8163.
20. Lavin MF and Kozlov S. ATM activation and DNA damage response. *Cell cycle*. 2007; 6:931-942.
21. Wilson KA and Stern DF. NFB1/MDC1, 53BP1 and BRCA1 have both redundant and unique roles in the ATM pathway. *Cell Cycle*. 2008; 7:3584-3594.
22. Hirao A, Kong Y-Y, Matsuoka S, Wakeham A, Ruland J, Yoshida H, Liu D, Elledge SJ and Mak TW. DNA damage-induced activation of p53 by the checkpoint kinase Chk2. *Science*. 2000; 287:1824-1827.
23. Yu Q, La Rose J, Zhang H, Takemura H, Kohn KW and Pommier Y. UCN-01 inhibits p53 up-regulation and abrogates  $\gamma$ -radiation-induced G2-M checkpoint independently of p53 by targeting both of the checkpoint kinases, Chk2 and Chk1. *Cancer Res*. 2002; 62:5743-5748.
24. Verma R. Aflatoxin cause DNA damage. *Int J Hum Genet*. 2004; 4:231.
25. Gursoy-Yuzugullu O, Yuzugullu H, Yilmaz M and Ozturk M. Aflatoxin genotoxicity is associated with a defective DNA damage response bypassing p53 activation. *Liver International*. 2011; 31:561-571.
26. Elledge SJ. Cell cycle checkpoints: preventing an identity crisis. *Science*. 1996; 274:1664-1672.
27. Piette J, Neel H and Marechal V. Mdm2: keeping p53 under control. *Oncogene*. 1997; 15:1001-1010.
28. Bunz F, Dutriaux A, Lengauer C, Waldman T, Zhou S, Brown J, Sedivy J, Kinzler K and Vogelstein B. Requirement for p53 and p21 to sustain G2 arrest after DNA damage. *Science*. 1998; 282:1497-1501.
29. Quaas M, Müller GA and Engeland K. p53 can repress transcription of cell cycle genes through a p21WAF1/CIP1-dependent switch from MMB to DREAM protein complex binding at CHR promoter elements. *Cell Cycle*. 2012; 11:4661-4672.
30. Poluha W, Poluha DK, Chang B, Crosbie NE, Schonhoff CM, Kilpatrick DL and Ross AH. The cyclin-dependent kinase inhibitor p21 (WAF1) is required for survival of differentiating neuroblastoma cells. *Mol Cell Biol*. 1996; 16:1335-1341.
31. Ando T, Kawabe T, Ohara H, Ducommun B, Itoh M and Okamoto T. Involvement of the interaction between p21 and proliferating cell nuclear antigen for the maintenance of G2/M arrest after DNA damage. *J Biol Chem*. 2001; 276:42971-42977.
32. Zhang H, Xiong Y and Beach D. Proliferating cell nuclear antigen and p21 are components of multiple cell cycle kinase complexes. *Mol Biol Cell*. 1993; 4:897-906.
33. Kelman Z. PCNA: structure, functions and interactions. *Oncogene*. 1997; 14.
34. Maga G and Hübscher U. Proliferating cell nuclear antigen (PCNA): a dancer with many partners. *J Cell Sci*. 2003; 116:3051-3060.
35. Bravo R, Frank R, Blundell PA and Macdonald-Bravo H. Cyclin/PCNA is the auxiliary protein of DNA polymerase- $\delta$ . *Nature*. 1987; 326:515-517.
36. Bulavin DV, Higashimoto Y, Popoff IJ, Gaarde WA, Basur V, Potapova O, Appella E and Fornace AJ. Initiation of a G2/M checkpoint after ultraviolet radiation requires p38 kinase. *Nature*. 2001; 411:102-107.
37. Syam S, Bustamam A, Abdullah R, Sukari MA, Hashim NM, Ghaderian M, Rahmani M, Mohan S, Abdelwahab SI and Ali HM.  $\beta$ -Mangostin induces p53-dependent G2/M cell cycle arrest and apoptosis through ROS mediated mitochondrial pathway and Nf $\kappa$ B suppression in MCF-7 cells. *J Funct Foods*. 2014; 6:290-304.
38. Chang C-H, Yu F-Y, Wu T-S, Wang L-T and Liu B-H. Mycotoxin citrinin induced cell cycle G2/M arrest and numerical chromosomaaberration associated with disruption of microtubule formation in human cells. *Toxicol Sci*. 2010; 119:84-92.
39. Yang H, Chung DH, Kim YB, Choi YH and Moon Y. Ribotoxic mycotoxin deoxynivalenol induces G2/M cell cycle arrest *via* p21 Cip/WAF1 mRNA stabilization in human epithelial cells. *Toxicol*. 2008; 243:145-154.
40. Cui J, Xing L, Li Z, Wu S, Wang J, Liu J, Wang J, Yan X and Zhang X. Ochratoxin A induces G 2 phase arrest in human gastric epithelium GES-1 cells *in vitro*. *Toxicol Lett*. 2010; 193:152-158.
41. Nigg EA. Mitotic kinases as regulators of cell division and its checkpoints. *Nat Rev Mol Cell Bio*. 2001; 2:21-32.
42. Bartek J and Lukas J. Chk1 and Chk2 kinases in checkpoint control and cancer. *Cancer Cell*. 2003; 3:421-429.
43. Smits VA, Klompmaker R, Vallenius T, Rijkssen G, Mäkelä TP and Medema RH. p21 inhibits Thr161 phosphorylation of Cdc2 to enforce the G2 DNA damage checkpoint. *J Biol Chem*. 2000; 275:30638-30643.
44. Dale N. National Research Council Nutrient Requirements of Poultry-Ninth Revised Edition (1994). *J Appl Poultry Res*. 1994; 3:101-101.
45. Kaoud HA. Innovative methods for the amelioration of aflatoxin (AFB1) effect in broiler chicks. *Sci J Appl Res*. 2013; 1:15-19.
46. Chen T, Cui H, Cui Y, Bai C, Gong T and Peng X. Cell-cycle blockage associated with increased apoptotic cells in the thymus of chickens fed on diets high in fluorine. *Hum Exp Toxicol*. 2011; 30:685-692.

47. Fang J, Cui H, Peng X, Chen Z, He M and Tang L. Developmental changes in cell proliferation and apoptosis in the normal duck thymus. *Anat Histol Embryol.* 2011; 40:457-465.
48. Wu B, Cui H, Peng X, Fang J, Zuo Z, Deng J and Huang J. Dietary nickel chloride induces oxidative stress, apoptosis and alters Bax/Bcl-2 and caspase-3 mRNA expression in the cecal tonsil of broilers. *Food Chem Toxicol.* 2014; 63:18-29.
49. Livak KJ and Schmittgen TD. Analysis of relative gene expression data using real-time quantitative PCR and the 2- $\Delta\Delta$ CT method. *Methods.* 2001; 25:402-408.